Available online at www.sciencedirect.com
ScienceDirect
Catalysis Today 132 (2008) 58–62
CATALYSIS TODAY
www.elsevier.com/locate/cattod

Preparation of $H_5PMo_{10}V_2O_{40}$ catalyst immobilized on nitrogen-containing mesostructured cellular foam carbon (N-MCF-C) and its application to the vapor-phase oxidation of benzyl alcohol

Heesoo Kim [a], Ji Chul Jung [a], Dong Ryul Park [a], Howon Lee [a], Joohyung Lee [a], Sang Hee Lee [a], Sung-Hyeon Baeck [b], Kwan-Young Lee [c], Jongheop Yi [a], In Kyu Song [a,*]

[a] *School of Chemical and Biological Engineering, Institute of Chemical Processes, Seoul National University, Shinlim-dong, Kwanak-ku, Seoul 151-744, Republic of Korea*
[b] *Department of Chemical Engineering, Inha University, Incheon 402-751, Republic of Korea*
[c] *Department of Chemical and Biological Engineering, Korea University, Annam-dong, Sungbuk-ku, Seoul 136-701, Republic of Korea*

Available online 16 January 2008

Abstract

Nitrogen-containing mesostructured cellular foam carbon (N-MCF-C) was synthesized by a templating method using mesostructured cellular foam silica (MCF-S) and polypyrrole as a templating agent and a carbon precursor, respectively. The N-MCF-C was then modified to have a positive charge, and thus, to provide a site for the immobilization of $[PMo_{10}V_2O_{40}]^{5-}$. By taking advantage of the overall negative charge of $[PMo_{10}V_2O_{40}]^{5-}$, $H_5PMo_{10}V_2O_{40}$ ($PMo_{10}V_2$) catalyst was chemically immobilized on the N-MCF-C support as a charge-matching component. Characterization results showed that the $PMo_{10}V_2$ catalyst was finely dispersed on the N-MCF-C support via strong chemical interaction, and that the pore structure of N-MCF-C was still maintained even after the immobilization of $PMo_{10}V_2$. In the vapor-phase oxidation of benzyl alcohol, the $PMo_{10}V_2$/N-MCF-C catalyst showed a higher conversion and a higher oxidation activity (formation of benzaldehyde) than the unsupported $PMo_{10}V_2$ and $PMo_{10}V_2$/MCF-S catalysts.

Keywords: Heteropolyacid; Nitrogen-containing mesostructured cellular foam carbon; Chemical immobilization; Benzyl alcohol oxidation

1. Introduction

Heteropolyacids (HPAs) are early transition-metal oxygen anion clusters that have found successful applications in homogeneous and heterogeneous catalysis [1–3]. Among various HPA structural classes, the Keggin [4] HPAs have been used as commercial catalysts [1–3]. The Keggin HPA has a soccer ball shape with a molecular size of ca. 1 nm [5]. One of the great advantages of HPA catalysts is that their acid–base and redox properties can be tuned in a systematic way by changing the identity of counter-cation, central heteroatom, and framework polyatom [1–3].

A disadvantage of HPA catalysts, however, is that their surface area is very low ($<10\ m^2/g$). To overcome the low surface area, HPA catalysts have been supported on various inorganic materials by a conventional impregnation method [6]. Another promising approach for increasing the surface area of HPA catalysts is to take advantage of the overall negative charge of heteropolyanions. By this method, HPAs have been immobilized on polymer materials such as poly-4-vinylpyridine [7], polyaniline [8], and polystyrene [9]. Although such an attempt utilizing inorganic supporting materials has been restricted due to the difficulty in forming a positive charge on the inorganic supporting materials, HPAs have also been

* Corresponding author. Tel.: +82 2 880 9227; fax: +82 2 889 7415.
E-mail address: inksong@snu.ac.kr (I.K. Song).

0920-5861/$ – see front matter © 2007 Elsevier B.V. All rights reserved.
doi:10.1016/j.cattod.2007.12.004

successfully immobilized on inorganic mesoporous materials such as HMS [10], MCM-41 [11], SBA-15 [12], CMK-3 [13], and mesostructured cellular foam silica [14] through a surface modification process.

Mesoporous carbon materials have high surface area, large pore volume, and uniform pore size distribution [15]. In spite of the difficulty in forming a positive charge on the mesoporous carbon materials, mesoporous carbon materials still have merit as catalyst supports due to their excellent thermal stability and controllable textural properties. If mesoporous carbon materials are modified to have a positive charge by an easy method, they can serve as efficient supports for HPA catalyst.

In this work, nitrogen-containing mesostructured cellular foam carbon (N-MCF-C) was synthesized by a templating method using mesostructured cellular foam silica (MCF-S) and polypyrrole as a templating agent and a carbon precursor, respectively. The N-MCF-C was then modified to have a positive charge for the immobilization of $[PMo_{10}V_2O_{40}]^{5-}$. By taking advantage of the overall negative charge of $[PMo_{10}V_2O_{40}]^{5-}$, $H_5PMo_{10}V_2O_{40}$ ($PMo_{10}V_2$) catalyst was chemically immobilized on the N-MCF-C support as a charge-matching component. The $PMo_{10}V_2$/N-MCF-C catalyst was characterized and applied to the vapor-phase oxidation of benzyl alcohol.

2. Experimental

MCF-S was synthesized for use as a templating material for N-MCF-C according to the method in the literature [16]. N-MCF-C was synthesized as follows. $FeCl_3$ (1.0 g) dissolved in an aqueous HCl solution (1.5 ml, 1.0 M) was impregnated on the MCF-S (1.0 g) by an incipient wetness method. The yellow-colored slurry was dried at 100 °C in a convection oven. The resulting solid was reacted with pyrrole monomer (0.5 g) at room temperature under vacuum for the polymerization of pyrrole. The composite of MCF-S and polypyrrole was dried at 80 °C, and it was then carbonized at 900 °C for 5 h in a stream of nitrogen (40 ml/min). The silica template was removed by the treatment with HF and HNO_3. After washing the solid with de-ionized water several times, the resulting solid was finally dried at 100 °C in a convection oven to yield the N-MCF-C [17].

Fig. 1 shows the schematic procedures for the surface modification of N-MCF-C and the subsequent immobilization of $PMo_{10}V_2$ on the N-MCF-C. N-MCF-C (1.0 g) was activated by flowing hydrogen (10 ml/min) at 150 °C for 2 h to create amine groups on the surface of the N-MCF-C. The activated N-MCF-C was then treated with an aqueous HCl solution (pH < 4) for 12 h to form a positive charge. The resulting N-MCF-C was washed with de-ionized water several times, and subsequently, dried overnight at 100 °C to yield the surface-modified N-MCF-C. For the preparation of $PMo_{10}V_2$/N-MCF-C, $PMo_{10}V_2$ (1.0 g) and surface-modified N-MCF-C (1.0 g) were dissolved in acetonitrile (100 ml). The pH of the mixed slurry was maintained below 2.0 using an aqueous HCl solution. The slurry was stirred for 24 h at room temperature for the immobilization of $PMo_{10}V_2$ on the surface-modified N-MCF-C. After the solid product was recovered by filtration, it was washed with de-ionized water several times until the washing solvent became colorless. The solid product was dried at 100 °C overnight and calcined at 200 °C for 3 h to yield the $PMo_{10}V_2$/N-MCF-C. For comparison, $PMo_{10}V_2$ supported on MCF-S was also prepared by an impregnation method ($PMo_{10}V_2$/MCF-S).

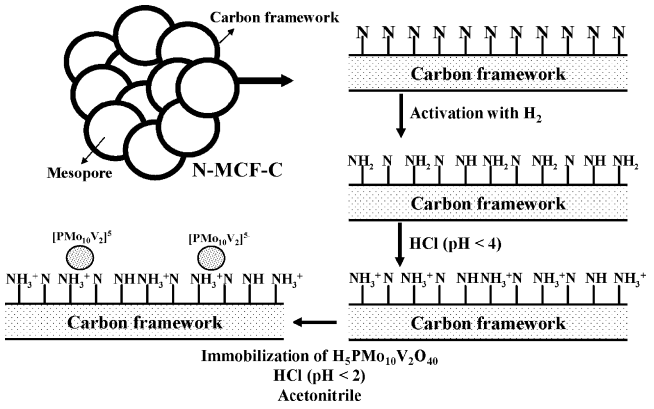

Fig. 1. Schematic procedures for the surface modification of N-MCF-C and the subsequent immobilization of $PMo_{10}V_2$ on the N-MCF-C.

N_2 adsorption–desorption isotherms of support and supported catalyst were obtained with an ASAP-2010 instrument (Micromeritics). Surface areas and pore volumes of the prepared samples were calculated using the BET equation and the BJH model, respectively. Nitrogen contents were determined by CHN elemental analyses (EC Instrument, EA1110). $PMo_{10}V_2$ content in the $PMo_{10}V_2$/N-MCF-C was measured by ICP-AES analyses (Shimadz, ICP-1000IV). Support and supported catalyst were further characterized by TEM (Jeol, JEM-200CX), XRD (Rigaku, D-MAX2500-PC), FT-IR (Nicolet, Impact 410), and ^{31}P CP-MAS NMR (Brunker, AVANCE 400 WB, DSX-400) analyses.

The vapor-phase oxidation of benzyl alcohol was carried out in a continuous flow fixed-bed reactor at atmospheric pressure. Unsupported $PMo_{10}V_2$, $PMo_{10}V_2$/MCF-S or $PMo_{10}V_2$/N-MCF-C (40 mg on $PMo_{10}V_2$ basis) was charged into a tubular quartz reactor, and then it was pretreated with a mixed stream of nitrogen (10 ml/min) and oxygen (10 ml/min) at 280 °C for 1 h. Benzyl alcohol (2.90×10^{-3} mol/h) was sufficiently vaporized by passing through a pre-heating zone and continuously fed into the reactor together with oxygen (10 ml/min) and nitrogen carrier (10 ml/min). The contact time was maintained at 13.8 g $PMo_{10}V_2$-h/benzyl alcohol-mol. The catalytic reaction was carried out at 260 °C for 5 h. The reaction products were periodically sampled and analyzed with an on-line gas chromatograph (HP 5890 II).

3. Results and discussion

Physical properties and chemical compositions of support and supported catalyst are listed in Table 1. The nitrogen content of N-MCF-C was 3.75 wt%, while that of $PMo_{10}V_2$/N-MCF-C was measured to be 2.86 wt%. The decreased nitrogen content of the $PMo_{10}V_2$/N-MCF-C was due to the loading of

Table 1
Physical properties and chemical compositions of support and supported catalyst

	BET surface area (m^2/g)	Pore volume (cm^3/g)	Nitrogen content (wt%)	$PMo_{10}V_2$ content (wt%)
N-MCF-C	718	1.21	3.75	–
$PMo_{10}V_2$/N-MCF-C	538	0.93	2.86	12.4
Bulk $PMo_{10}V_2$	4	–	–	–

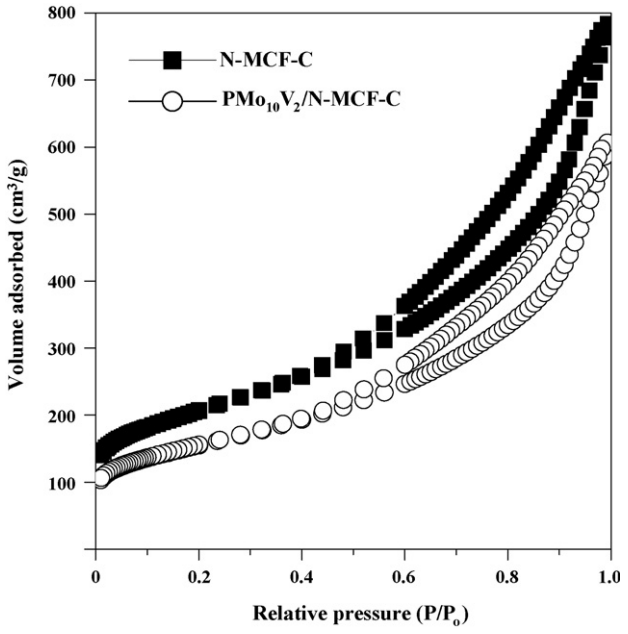

Fig. 2. N_2 adsorption–desorption isotherms of N-MCF-C and $PMo_{10}V_2$/N-MCF-C.

$PMo_{10}V_2$ on the N-MCF-C. The amount of $PMo_{10}V_2$ immobilized on the N-MCF-C was found to be 12.4 wt%. Surface area (= 718 m^2/g) and pore volume (= 1.21 cm^3/g) of N-MCF-C were slightly decreased upon immobilization of $PMo_{10}V_2$. However, the $PMo_{10}V_2$/N-MCF-C still retained relatively high surface area (= 538 m^2/g) and large pore volume (= 0.93 cm^3/g). An attempt has been made to immobilize $PMo_{10}V_2$ on the MCF-S. In this case, however, $PMo_{10}V_2$ was totally dissolved out during the washing step due to the absence of an anchoring site for $PMo_{10}V_2$ on the MCF-S. This indicates that nitrogen in the N-MCF-C played an important role in forming a nitrogen-derived functional group (amine group) for the immobilization of $PMo_{10}V_2$. Therefore, $PMo_{10}V_2$/MCF-S was prepared by an impregnation method for the purpose of comparison.

Fig. 2 shows the N_2 adsorption–desorption isotherms of N-MCF-C and $PMo_{10}V_2$/N-MCF-C. Both N-MCF-C and $PMo_{10}V_2$/N-MCF-C showed type IV isotherms and type H1 hysteresis loops. The main cell pore sizes of N-MCF-C and $PMo_{10}V_2$/N-MCF-C were in the range of 10–30 nm. These results indicate that the pore structure of N-MCF-C was still maintained even after the immobilization of $PMo_{10}V_2$.

Fig. 3 shows the TEM images of N-MCF-C and $PMo_{10}V_2$/N-MCF-C. Disordered pore arrays were clearly observed in both samples. The main cell pore diameters of both samples determined from TEM images were ca. 20 nm, in good agreement with the pore size distribution calculated from the BJH isotherm model. This result is also well consistent with the previous work [18] that reported the TEM images of MCF-C. It is noteworthy that there was no great difference in pore array and pore shape between N-MCF-C and $PMo_{10}V_2$/N-MCF-C. Once again, this result strongly supports that the pore structure of N-MCF-C was maintained even after the immobilization of $PMo_{10}V_2$. Furthermore, no visible evidence representing $PMo_{10}V_2$ species was found in the $PMo_{10}V_2$/N-MCF-C, indicating that $PMo_{10}V_2$ species were finely dispersed on the N-MCF-C support.

Fig. 4 shows the XRD patterns of unsupported $PMo_{10}V_2$, N-MCF-C, and $PMo_{10}V_2$/N-MCF-C. Unsupported $PMo_{10}V_2$ showed the characteristic XRD peaks of the HPA. On the other hand, N-MCF-C support showed the characteristic diffraction peaks for (0 0 2) and (1 0 1) planes at around $2\theta = 26.3^\circ$ and 43°, respectively, indicating that the N-MCF-C retained a graphitic structure. However, $PMo_{10}V_2$/N-MCF-C catalyst exhibited no characteristic XRD pattern of $PMo_{10}V_2$ but showed almost the same XRD pattern as N-MCF-C, even

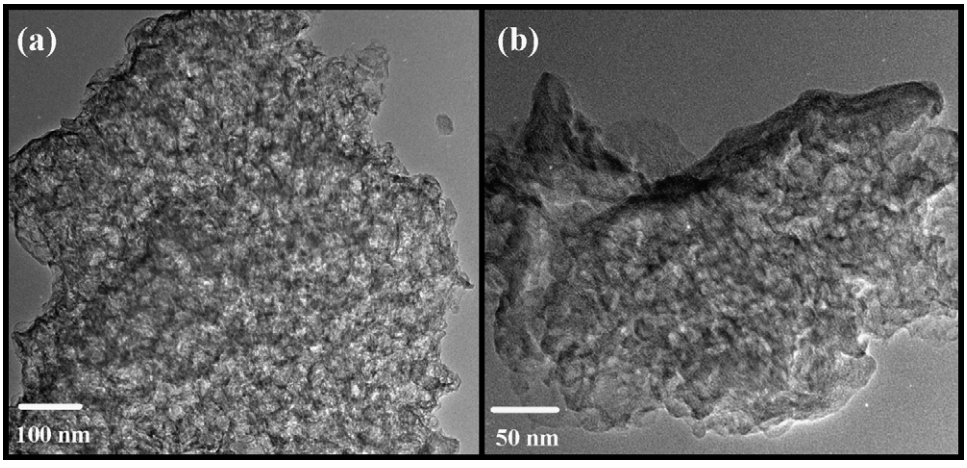

Fig. 3. TEM images of (a) N-MCF-C and (b) $PMo_{10}V_2$/N-MCF-C.

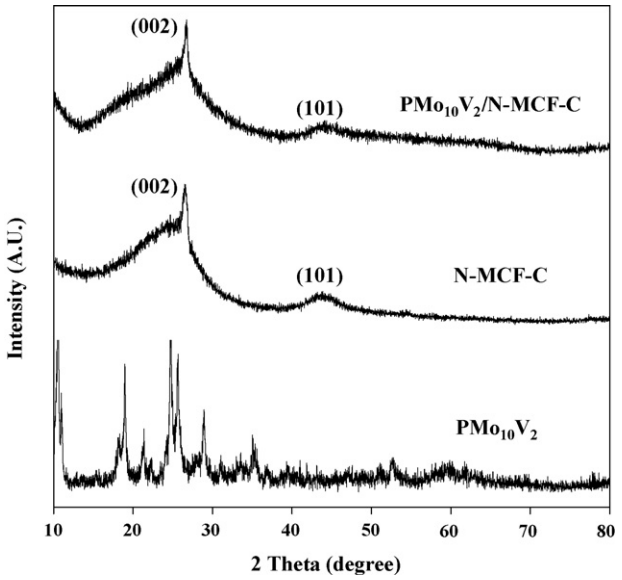

Fig. 4. XRD patterns of unsupported $PMo_{10}V_2$, N-MCF-C, and $PMo_{10}V_2$/N-MCF-C.

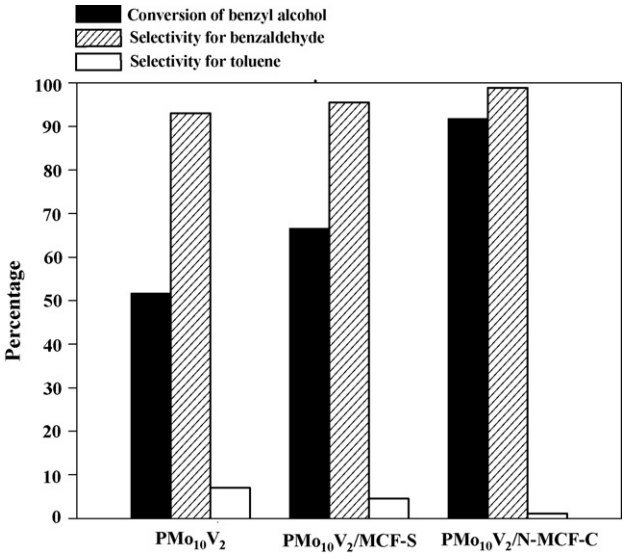

Fig. 5. Catalytic performance of unsupported $PMo_{10}V_2$, $PMo_{10}V_2$/MCF-S, and $PMo_{10}V_2$/N-MCF-C in the vapor-phase oxidation of benzyl alcohol at 260 °C after a 5-h reaction.

though 12.4 wt% $PMo_{10}V_2$ was loaded in the $PMo_{10}V_2$/N-MCF-C catalyst. This result indicates that $PMo_{10}V_2$ species were not in a crystal state but in an amorphous-like state, demonstrating that $PMo_{10}V_2$ species were finely dispersed on the N-MCF-C support.

Chemical immobilization of $PMo_{10}V_2$ on the N-MCF-C was confirmed by FT-IR analyses (FT-IR spectra of the samples are not shown here). The four characteristic IR bands of $PMo_{10}V_2$ appeared at 1063, 964, 873, and 794 cm^{-1}, which are assigned to P–O, M(polyatom)=O, interoctahedral M–O–M, and intra-octahedral M–O–M bands, respectively. On the other hand, N-MCF-C showed no characteristic IR bands within the range of 700–1200 cm^{-1} due to the strong absorbance of the carbon material by infrared beam. The characteristic IR bands of $PMo_{10}V_2$ in the $PMo_{10}V_2$/N-MCF-C catalyst were observed at 1065 (P–O band), 895 (interoctahedral M–O–M band), and 800 (intra-octahedral M–O–M band) cm^{-1}, but M=O band was not clearly resolved. In other words, the characteristic IR bands of $PMo_{10}V_2$ in the $PMo_{10}V_2$/N-MCF-C appeared at slightly shifted positions compared to those of the unsupported $PMo_{10}V_2$. This result indicates that $PMo_{10}V_2$ was successfully immobilized on the N-MCF-C via strong chemical interaction between two components. Chemical immobilization of $PMo_{10}V_2$ on the N-MCF-C was further confirmed by ^{31}P CP-MAS NMR analyses (^{31}P CP-MAS NMR spectra of the samples are not presented here). Unsupported $PMo_{10}V_2$ showed a chemical shift at $\delta = -3.9$ ppm. This resonance peak corresponds to the structural phosphorus in the $PMo_{10}V_2$, in good agreement with the previous report [3]. On the other hand, the chemical shift of $PMo_{10}V_2$/N-MCF-C appeared at $\delta = -7.2$ ppm. This result indicates that the surroundings of phosphorous atom were remarkably changed, suggesting that $PMo_{10}V_2$ was successfully immobilized on the N-MCF-C support via strong chemical interaction.

Fig. 5 shows the catalytic performance of unsupported $PMo_{10}V_2$, $PMo_{10}V_2$/MCF-S, and $PMo_{10}V_2$/N-MCF-C in the vapor-phase oxidation of benzyl alcohol at 260 °C after a 5-h reaction. The conversion of benzyl alcohol increased in the order of $PMo_{10}V_2 < PMo_{10}V_2$/MCF-S $< PMo_{10}V_2$/N-MCF-C. The $PMo_{10}V_2$/MCF-S catalyst showed a higher conversion than the unsupported $PMo_{10}V_2$ catalyst, due to the relatively fine dispersion of $PMo_{10}V_2$ species on the MCF-S. The enhanced catalytic performance of $PMo_{10}V_2$/N-MCF-C was due to the fine dispersion of $PMo_{10}V_2$ on the surface of N-MCF-C formed via chemical immobilization. It is known that benzaldehyde is formed by the oxidation catalytic function of HPA, while toluene is produced by the acid catalytic function of HPA [19]. It should be noted that the $PMo_{10}V_2$/N-MCF-C catalyst exhibited an enhanced oxidation catalytic activity (formation of benzaldehyde) and a suppressed acid catalytic activity (formation of toluene) compared to the other two catalysts. Unsupported $PMo_{10}V_2$ and $PMo_{10}V_2$/MCF-S catalysts retain their own acid and oxidation catalytic functions. Unlike the bulk $PMo_{10}V_2$ and $PMo_{10}V_2$/MCF-S, $PMo_{10}V_2$ in the $PMo_{10}V_2$/N-MCF-C was chemically immobilized on the positive site ($-NH_3^+$) of N-MCF-C by sacrificing its protons. As attempted in this work, it is believed that the $[PMo_{10}V_2O_{40}]^{5-}$ was finely and chemically immobilized on the N-MCF-C as a charge-matching component by losing protons (acid sites). Therefore, the $PMo_{10}V_2$/N-MCF-C catalyst showed an enhanced oxidation catalytic activity and a suppressed acid catalytic activity compared to the bulk $PMo_{10}V_2$ and $PMo_{10}V_2$/MCF-S catalysts.

4. Conclusions

N-MCF-C was synthesized by a templating method using MCF-S and polypyrrole as a templating agent and a carbon precursor, respectively. The N-MCF-C was then modified to have a positive charge for the immobilization of $[PMo_{10}V_2O_{40}]^{5-}$. By taking advantage of the overall negative

charge of $[PMo_{10}V_2O_{40}]^{5-}$, $PMo_{10}V_2$ catalyst was immobilized on the N-MCF-C support as a charge-matching component. Nitrogen in the N-MCF-C played an important role in forming a nitrogen-derived functional group (amine group) for the immobilization of $PMo_{10}V_2$. It was found that $PMo_{10}V_2$ was finely immobilized on the N-MCF-C support via strong chemical interaction. The pore structure of N-MCF-C was still maintained even after the immobilization of $PMo_{10}V_2$. In the vapor-phase oxidation of benzyl alcohol, the $PMo_{10}V_2$/N-MCF-C catalyst showed a higher conversion than the unsupported $PMo_{10}V_2$ and $PMo_{10}V_2$/MCF-S catalysts, due to the fine dispersion of $PMo_{10}V_2$ on the surface of N-MCF-C formed via chemical immobilization. Furthermore, the $PMo_{10}V_2$/N-MCF-C catalyst exhibited an enhanced oxidation catalytic activity (formation of benzaldehyde) and a suppressed acid catalytic activity (formation of toluene) compared to the $PMo_{10}V_2$ and $PMo_{10}V_2$/MCF-S catalysts.

Acknowledgement

The authors wish to acknowledge support from the Korea Science and Engineering Foundation (KOSEF R01-2004-000-10502-0).

References

[1] I.V. Kozhevnikov, Catal. Rev. Sci. Eng. 37 (1995) 311.
[2] C.L. Hill, C.M. Prosser-McCartha, Coord. Chem. Rev. 143 (1995) 407.
[3] T. Okuhara, N. Mizuno, M. Misono, Adv. Catal. 41 (1996) 113.
[4] J.F. Keggin, Nature 131 (1933) 908.
[5] I.K. Song, M.A. Barteau, Korean J. Chem. Eng. 19 (2002) 567.
[6] N.-Y. He, C.-S. Woo, H.-G. Kim, H.-I. Lee, Appl. Catal. A 281 (2005) 167.
[7] K. Nomiya, H. Murasaki, M. Miwa, Polyhedron 5 (1986) 1031.
[8] M. Hasik, W. Turek, E. Stochmal, M. Lapowski, A. Proń, J. Catal. 147 (1994) 544.
[9] H. Kim, J.C. Jung, S.H. Yeom, K.-Y. Lee, I.K. Song, J. Mol. Catal. A 248 (2006) 21.
[10] Y. Liu, K. Murata, M. Inaba, J. Mol. Catal. A 256 (2006) 247.
[11] W. Kaleta, K. Nowińska, Chem. Commun. (2001) 535.
[12] N.K. Kala Raj, S.S. Deshpande, R.H. Ingle, T. Raja, P. Manikandan, Catal. Lett. 98 (2004) 217.
[13] H. Kim, P. Kim, K.-Y. Lee, S.H. Yeom, J. Yi, I.K. Song, Catal. Today 111 (2006) 361.
[14] H. Kim, J.C. Jung, P. Kim, S.H. Yeom, K.-Y. Lee, I.K. Song, J. Mol. Catal. A 259 (2006) 150.
[15] J. Lee, S. Han, H. Kim, J.H. Koh, T. Hyeon, S.H. Moon, Catal. Today 86 (2003) 141.
[16] D. Zhao, J. Feng, Q. Huo, N. Melosh, G.H. Fredrickson, B.F. Chmelka, G.D. Stucky, Science 279 (1998) 548.
[17] A.B. Fuertes, T.A. Centeno, J. Mater. Chem. 15 (2005) 1079.
[18] J. Lee, K. Sohn, T. Hyeon, J. Am. Chem. Soc. 123 (2005) 5146.
[19] N. Lingaish, K.M. Reddy, N.S. Babu, K.N. Rao, I. Suryanarayana, P.S.S. Prasad, Catal. Commun. 7 (2006) 245.